CSMA 2017
13ème Colloque National en Calcul des Structures
15-19 Mai 2017, Presqu'île de Giens (Var)

Modeling and Identification of the constitutive behavior of magneto-rheological elastomers

JP. Voropaieff[1], L. Bodelot[1], K. Danas[1], N. Triantafyllidis[1,2]

[1] LMS, Ecole Polytechnique, {jean-pierre.voropaieff, laurence.bodelot}@polytechnique.edu, {kdanas, nick}@lms.polytechnique.fr
[2] Aerospace & Mechanical Engineering Department, The University of Michigan, USA

Abstract — In this paper, we study a class of active materials named magneto-rheological elastomers (MREs) with a main focus on their coupled magneto-mechanical response. Based on the theoretical framework proposed by Triantafyllidis [1], we develop the coupled magneto-mechanical constitutive laws in order to identify the corresponding model's material parameters. The experimental data, obtained with a novel experimental setup allowing tensile tests up to large strains and under high magnetic fields, provide the constitutive parameters needed as input for subsequent numerical simulations.

Keywords — Magneto-Rheological Elastomers (MRE), Experimental Characterization, Constitutive modeling, Parameter identification.

1 Motivations and Applications

Magneto-rheological elastomers (MREs) are smart materials composed of an elastomeric matrix filled with magnetic particles. The viscoelastic characteristics of the matrix combined with the magnetic properties of the particles allow these flexible composites to deform in response to a relatively low externally applied magnetic field. Moreover, different microscopic architecture (isotropic or transversely isotropic materials) can be obtained by adding only one step to the fabrication procedure.

The rapid response, the ability to choose the microstructure, the high level of deformations and the possibility to control these deformations by adjusting the field make these materials of special interest in modern engineering. Yet, the characterization of the magneto-mechanical properties for finite strains and high magnetic fields is still far from being optimal, thus limiting the efficient design of MRE-based devices.

2 Theoretical framework

In what follows, we present general constitutive laws for the coupled magneto-mechanical response. For a detailed derivation of the governing equations, the reader is referred to the work of Danas, Kankanala and Triantafyllidis ([1] and [2]). Of interest here is the determination of the specific free energy ψ that best fits the MRE experiments. Using the general theory of transversely isotropic functions, one obtains that the general form of the specific Helmholtz free energy is given by

$$\rho_0 \psi = W(I_1, I_2, I_3, I_4, I_5, I_6, I_7, I_8, I_9, I_{10}) \tag{1}$$

where I_i are ten independent invariants. Each of those invariants depend on $\mathbf{F}$ the deformation gradient, $\mathbf{m}$ the magnetization vector and the unit vector $\widehat{\mathbf{N}}$ which defines the initial orientation of the particle chains.

$$
\begin{aligned}
&I_1 = tr(\mathbf{F}^T \cdot \mathbf{F}), \quad I_2 = \frac{1}{2}\left[I_1^2 - tr(\mathbf{F}^T \cdot \mathbf{F})^2\right], \quad I_3 = det(\mathbf{F}^T \cdot \mathbf{F}) = J^2 \\
&I_4 = \widehat{\mathbf{N}} \cdot \mathbf{F}^T \cdot \mathbf{F} \cdot \widehat{\mathbf{N}}, \quad I_5 = \widehat{\mathbf{N}} \cdot (\mathbf{F}^T \cdot \mathbf{F})^2 \cdot \widehat{\mathbf{N}} \\
&I_6 = \mathbf{m} \cdot \mathbf{m}, \quad I_7 = \mathbf{m} \cdot \mathbf{F} \cdot \mathbf{F}^T \cdot \mathbf{m}, \quad I_8 = \mathbf{m} \cdot (\mathbf{F} \cdot \mathbf{F}^T)^2 \cdot \mathbf{m} \\
&I_9 = (\mathbf{m} \cdot \mathbf{F} \cdot \widehat{\mathbf{N}})^2, \quad I_{10} = (\mathbf{m} \cdot \mathbf{F} \cdot \widehat{\mathbf{N}})(\mathbf{m} \cdot \mathbf{F} \cdot \mathbf{F}^T \cdot \mathbf{F} \cdot \widehat{\mathbf{N}})
\end{aligned} \tag{2}
$$

Based on the work of Kankanala and Triantafyllidis [1], we get the following expressions for the Cauchy stress σ and the Eulerian magnetic intensity $\mathbf{h}$.

$$\sigma = \sigma^T = \rho \frac{\partial \psi}{\partial \mathbf{F}} \cdot \mathbf{F}^T + \mathbf{h}\mathbf{b} - \mu_0(\mathbf{h} \cdot \mathbf{m} + \frac{1}{2}\mathbf{h} \cdot \mathbf{h})\mathbf{I}, \quad \mu_0\mathbf{h} = \rho \frac{\partial \psi}{\partial \mathbf{m}}, \tag{3}$$

where ρ is the current material density and $\mathbf{b}$ is the Eulerian magnetic field. Based on those expressions, the energy function W is identified by use of experimental results (the experimental procedure is discussed in the following sections).

3 Experimental characterization

3.1 Fabrication of samples

In the perspective of obtaining a material in which magneto-mechanical coupling is optimal (i.e. largest deformation produced by the smallest magnetic field) for a possible application in tactile MRE interface, the selected matrix material is a very soft silicone elastomer. The filler phase is made of spherical iron particles with a median diameter of $3.5\,\mu m$. Those particles are magnetically "soft", meaning that they do not retain magnetization once the magnetic field is turned off.
During the fabrication process, the magnetic particles of micron size are added to the uncured elastomer constituents and the obtained compound is thoroughly mixed and degassed, before curing is conducted in a mold of the desired shape. Moreover, the presence or the absence of a magnetic field during curing gives the possibility to produce either transversely isotropic (due to the formation of chain-like particle structures) or isotropic samples, respectively.

When characterizing MREs, a uniform field distribution (both mechanical and magnetic) within the sample should be achieved since field gradients can lead to additional deformation of the material on top of the original magneto-rheological effect. Even if the externally applied field $\mathbf{b}_0$ is assumed to be perfectly uniform, the shape of the magnetized MRE sample can create field gradients within the specimen. Magneto-static field equations and the corresponding boundary conditions suggest that the magnetization $\mathbf{m}$ as well as the total magnetic field $\mathbf{b}$ are uniform within the body only for ellipsoids of revolution. As a result, in order to find a compromise between the homogeneity of mechanical and magnetic quantities, the samples used are composed of a cylindrical gage area made of MRE and terminated at both ends by an ellipsoidal cap fixed to non-magnetic heads (see Figure 1(b)).
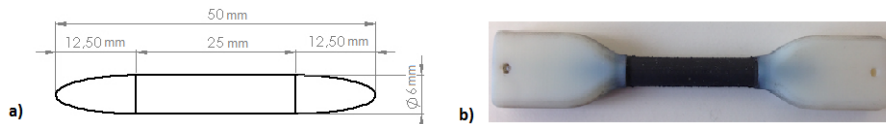

Figure 1:
(a): Cylindrical gage area terminated at both ends by an ellipsoidal cap (heads are not represented).
(b): Picture of the sample with non-magnetic heads.

3.2 Coupled magneto-mechanical testing

To obtain the macroscopic behavior of different MRE samples under coupled magneto-mechanical loading, we use a uniaxial tension setup integrated into a magnetic field (see Figure 2). First, we perform a uniaxial tension test up to large deformations with no magnetic fields. Then, coupled magneto-mechanical tests are conducted in which the sample is subjected to both an externally applied magnetic fied (up to 0.8T) and mechanical loads.
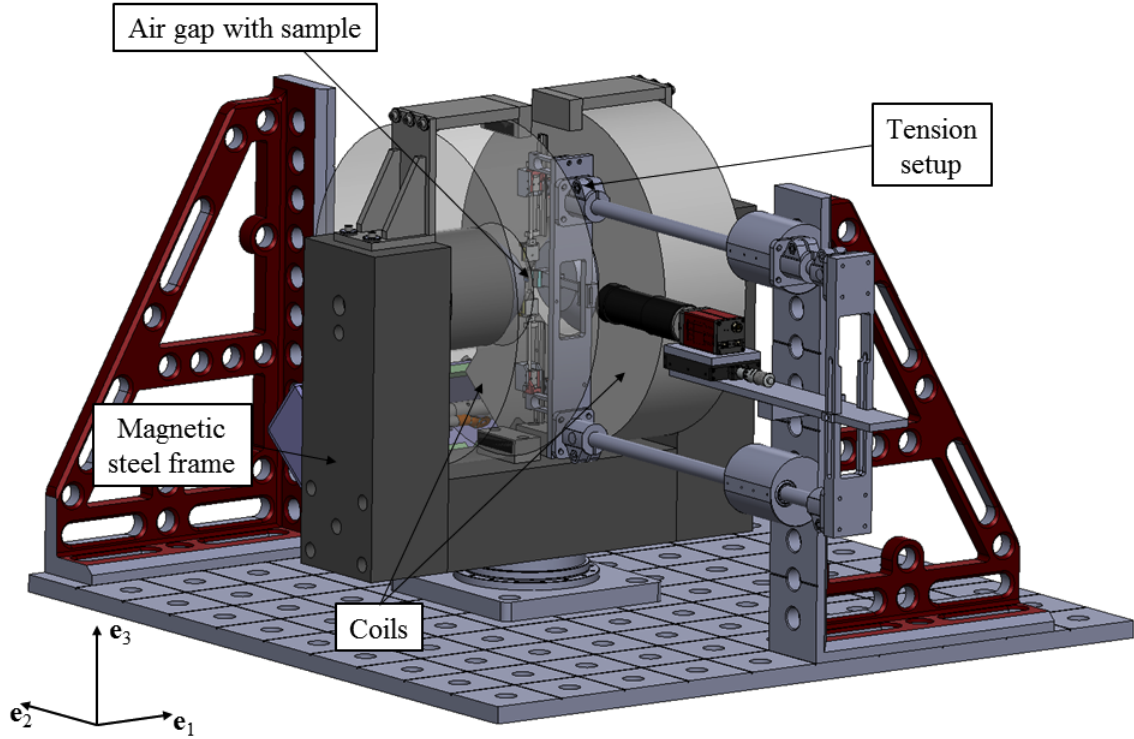

Figure 2: Tension setup integrated into a magnetic field

Mechanical strains in the gage area of the sample are measured via non-contact video extensometry and the force exerted on the sample during loading is measured by two single-point load cells. In situ magnetic field measurements are carried out with two transversal Hall probes. One probe (named probe h) comes behind the sample at its center (see Figure 3) and the second probe (named probe m) comes on the side of the sample (see Figure 3). Since the samples for the magnetic measurements have a nearly ellipsoidal MRE body, the **h**-field, the magnetization **m** and the total magnetic field **b**, are all assumed to be uniform within the material. This assumption is accurate at relatively moderate strains (eg. in the order of 10% which is the case in this study) but is expected to become less accurate at larger strains since in that case the shape diverges from an ellipsoid.

Due to the continuity of the tangential component of **h**, the Hall probe h placed at the back of the sample gives access to the total field $\mu_0 \mathbf{h}$ $[T]$ inside the material since the contribution of the magnetization **m** vanishes at that point. Due to the continuity of the normal component of **b**, the total magnetic field **b** $[T]$ inside the sample - now including the contribution of the total **h**-field (measured at the back) plus the contribution of the magnetization **m** - is measured by the lateral Hall probe m, which then gives access to the magnetization **m** inside the sample.

However, since the sensitive elements of the Hall probes cannot be placed exactly at the sample/air discontinuity interface due to geometrical limitations, we need to correct the measurement's systematic error due to the probe position. Expressions for the evolution of the magnetic field along direction $\mathbf{e}_1$ and $\mathbf{e}_2$ covering the discontinuity interface sample/air (see Figure 3b on the right)) are found analytically and checked experimentally.
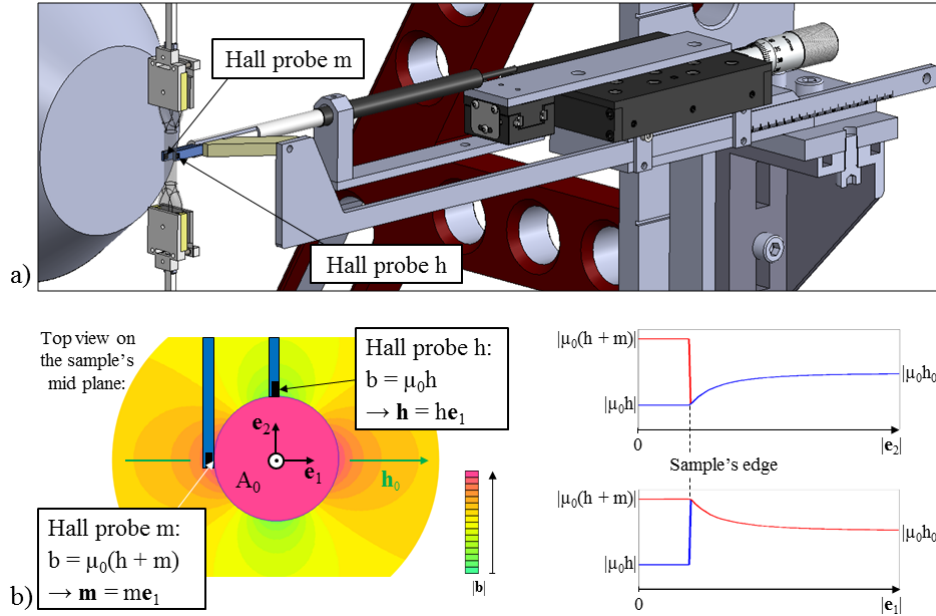
Figure 3:
(a): 3D view of the position of the Hall Probes.
(b): View from the top of the Hall probes (on the left) and evolution of the magnetic field outside the sample (on the right).

4 Parameter Identification

All the ingredients have been assembled to identify the material parameters that appear in the constitutive relations for isotropic (as well as for transversely isotropic) MRE continua. For the magneto-mechanical experimental data sets and the corresponding constitutive response depending on the material parameters p, the solution p* is determined on the basis of a least-squares optimization method (see Ogden et al. [3]). So far, the parameter identification procedure has been performed only for isotropic MRE and we detail this procedure in what follows.

4.1 Identification Procedure (for isotropic MRE)

The identification procedure for isotropic MRE is composed of two steps and pursues the following logic. First, the material parameters for a purely mechanical loading (which consists of a uniaxial tensile test along the axis of the sample in the absence of any magnetic field) are identified with the help of the corresponding experimental curves. The parameter identification results are shown in Figure 4 and we can see that the model can describe very well the experimental data.
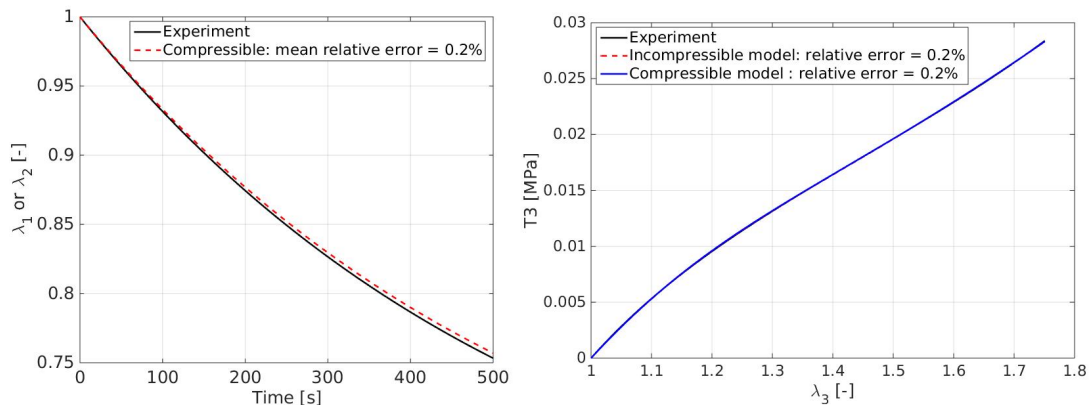

Figure 4: Fit of the stretch ratios λ_1 and λ_2 and the Traction T_3 (along the axis of the sample) for a uniaxial tensile test in which we impose a displacement along the axis of the sample .

4

Then, the magneto-mechanical response is identified keeping the constants found in the previous step. This time, we apply a mechanical prestretch along the axis of the sample that we keep constant during the entire test. In addition the sample is subjected to a magnetic field (that has its direction perpendicular to the axis of the sample). In order to analyze the magneto-mechanical couplings, both magnetic and mechanical quantities have to be measured during the sample deformation. As expected, the sample expands in the direction of the applied field and contracts in the other two transverse directions (see figure 5 on the left). As for the magnetization, it increases linearly with the applied magnetic field up to a certain point and then saturates (see figure 5 on the right). The value of the magnetization at saturation is denoted m_s.

The constitutive equations that apply in this case allow to find the missing material parameters related to magnetic invariants. With the help of Figure 5, we realize that once again the theoretical model can describe well enough the experiments (since we have a relative error of around 10%)
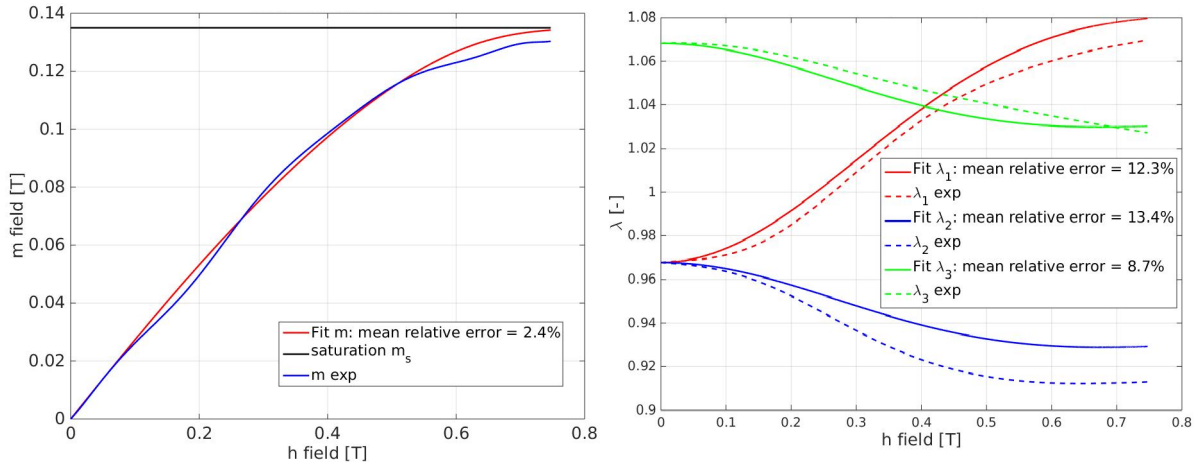

Figure 5: Fit of the stretch ratios and the **h-m** response

4.2 Predictive capabilities of the model

The predictive capabilities of the model are tested on a coupled magneto-mechanical test that is different from the previous one used in the fitting procedure. The test that we consider here is actually very similar to the one previously described except that the value of the mechanical prestretch is doubled. And as we see in Figure 6, the model can well predict the response of the material to that coupled loading.
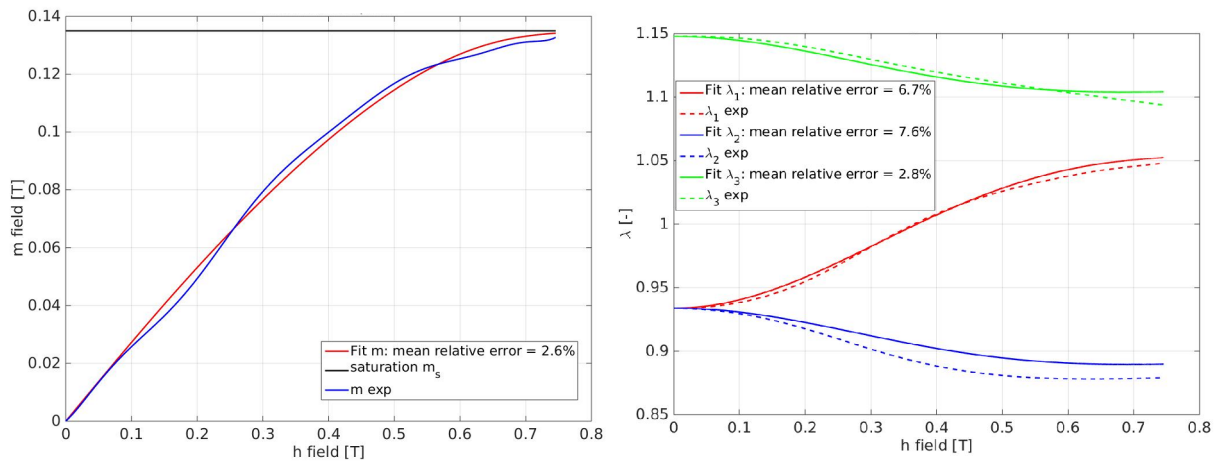

Figure 6: Prediction of the stretch ratios and the **h-m** response

References

[1] Kankanala, Triantafyllidis : *On finitely strained magnetorheological elastomers*, Journal of the Mechanics and Physics of Solids, 52:2869-2908, 2004.

[2] Danas, Kankanala, Triantafyllidis: *Experiments and modeling of iron-particle-filled magnetorheological elastomers*, Journal of the Mechanics and Physics of Solids, 60:120-138, 2012.

[3] R. Ogden et al: *Fitting hyperelastic models to experimental data*, Computational Mechanics, 484-502, 2004.